XLI CILAMCE
XLI Ibero-Latin American Congress on Computational Methods in Engineering
16-19 November, 2020 FOZ DO IGUAÇU PARANÁ - BRAZIL

Analysis of the elastoplastic behavior of porous microstructures under volumetric strains through a computational homogenization procedure

Wanderson F. Santos[1], Ayrton R. Ferreira[1], Sérgio P. B. Proença[1]

[1]*São Carlos School of Engineering, University of São Paulo*
Av. Trab. São Carlense, 13566-590, São Carlos, São Paulo, Brazil
wanderson_santos@usp.br, ayrton.ferreira@usp.br, persival@sc.usp.br

Abstract. The rupture processes in ductile materials such as metals and alloys occur by concentration of plastic strains around impurities in the microstructure. Therefore, the formulation of realistic constitutive models for these materials requires consideration of the effects of this heterogeneity on the distribution of stresses and strains at the microscale. These impurities are generally considered as voids due to the tendency of detaching from the surrounding matrix during the deformation process towards rupture. Moreover, different simplifications of the morphology of both void and matrix portion around it may imply different constitutive responses for identical load situations. Constitutive responses of porous materials can be constructed through computational homogenization procedure considering the behavior of representative volume elements (RVE). In this context, the present paper examines three different geometric configurations of ductile porous media RVE's subjected to volumetric strains. The matrix of each RVE is considered to be perfectly elastoplastic undergoing small strains regimes. The homogenized constitutive responses of the RVEs are obtained by averaging the stress and strain fields computed by Finite Element Method (FEM) analyses. The results hereby presented emphasize the determinant influence of the studied morphologies on the constitutive responses as the load level approaches the rupture regime.

Keywords: Metals and alloys, Ductile rupture, Computational homogenization, Micromechanics.

1 Introduction

Ductile rupture in metals and alloys is strongly related to the presence of voids in the material microstructure. Taking such (micro)voids into account in mechanical analyses requires more complex constitutive models to capture the material behavior. In order to obtain more representative answers to this class of problems, studies on the microscale become attractive by allowing to analyze in more detail the influence of heterogeneities and voids. However, several studies investigate macroscopically the rupture of porous ductile media using homogenization techniques based on low scales results obtained from FEM simulations. Next, one cite some recent works on this approach, which os also the subject of the present paper.

Fritzen et al. [1] employed a computational homogenization procedure to obtain the plastic collapse of cubic RVE's with multiple spherical voids randomly distributed within the matrix. Khdir et al. [2] assessed the rupture of cubic cells with multiple spheroidal voids randomly oriented within the matrix. Both works used 3D numerical simulations based on FEM to obtain microscopic fields.

Keralavarma [3] used computational homogenization with results obtained by 3D FEM analyses of RVEs to validate a plastic model of porous materials. The model is developed in a multi-surface approach and includes the localized and diffuse modes of plasticity on the microscale. In the context of numerical simulations, an additional analysis of the influence of the void geometry was performed by comparing the influence of a spherical void and a cubic void, each one within a cubic portion of matrix.

Another recent work on computational homogenization of RVEs simulated with FEM is Carvalho et al. [4]. In this case, the influence of the void morphology in 3D RVEs was evaluated with the nonlinear hypothesis of finite strains. The focus was on studying centered ellipsoidal voids on cube-shaped RVE's. Different boundary conditions were applied to the RVEs: (i) linear boundary displacements (upper bound); (ii) uniform boundary traction (lower bound); and (iii) periodic boundary fluctuations.

Dæhli et al. [5] obtained the homogenized behavior of porous isotropic ductile solids with matrix dependent on the second and third stress invariants. In their approach, the matrix is governed by the Hershey-Hosford criterion

(Hershey [6] and Hosford [7]). More specifically, numerical limit analyses were performed with FEM. The first analysis is based on the kinematic Gurson's test field (see details in Benallal [8]). The second analysis consists of a simple heuristic extension of Gurson's field (see details in Dæhli et al. [9]). RVE's with spherical and cubic morphologies were also compared.

The present work presents a computational homogenization procedure to study the ductile rupture of porous isotropic solids with a matrix governed by von Mises yield criterion. The influence of RVE morphology on the constitutive response is evaluated with the consideration of different geometries for it, as well the voids themselves. With the application of convenient boundary conditions, RVE's are subjected to volumetric strains and simulated through three-dimensional numerical analyses based on FEM. Finally, the microscopic fields obtained numerically (stresses and strains) are submitted to an average-based homogenization approach.

2 Basic concepts of the average-based homogenization theory

Within the scope of homogenization theories, fields in the macroscale (continuous) are obtained by averaging fields in the microscale (RVE):

$$\boldsymbol{E} = \frac{1}{V}\int_V \boldsymbol{\varepsilon} dV = <\boldsymbol{\varepsilon}>, \tag{1}$$

$$\boldsymbol{\Sigma} = \frac{1}{V}\int_V \boldsymbol{\sigma} dV = <\boldsymbol{\sigma}>, \tag{2}$$

where $\boldsymbol{\Sigma}$ and $\boldsymbol{E}$ are macroscopic total stress and strain fields, respectively; $\boldsymbol{\sigma}$ and $\boldsymbol{\varepsilon}$ are microscopic total stress and strain fields, respectively; $<>$ indicates volume average; and V consists of the total initial volume occupied by the RVE.

The association between the microscale and macroscale is established by the Hill-Mandel principle, based on the works of Hill [10] and Mandel [11]. In summary, this principle assumes the equivalence between amount of strain energy on both scales:

$$\boldsymbol{\Sigma} : \boldsymbol{E} = \frac{1}{V}\int_V \boldsymbol{\sigma} : \boldsymbol{\varepsilon} dV = <\boldsymbol{\sigma} : \boldsymbol{\varepsilon}> . \tag{3}$$

In the context of the present work, let us consider a porous material represented by an RVE (total volume V) composed by simple void (volume V_v) inserted in a matrix (volume $V_m = V - V_v$). Assuming compatibility between displacements and strains, after application of the Divergence Theorem to the void portion of the total volume, the following expressions can be obtained for the homogenized total stress and strain fields:

$$<\boldsymbol{\varepsilon}> = \frac{1}{V}\left[\int_{V_m} \boldsymbol{\varepsilon} dV + \frac{1}{2}\int_{\partial V_v} (\boldsymbol{u}\otimes\boldsymbol{n} + \boldsymbol{n}\otimes\boldsymbol{u})\, dS\right], \tag{4}$$

$$<\boldsymbol{\sigma}> = \frac{1}{V}\left[\int_{V_m} \boldsymbol{\sigma} dV + \int_{\partial V_v} (\boldsymbol{\sigma}\cdot\boldsymbol{n})\otimes\boldsymbol{x} dS\right], \tag{5}$$

where $\boldsymbol{n}$ is the normal versor at the surface of the void; $\boldsymbol{u}$ is the displacement vector; $\boldsymbol{x}$ is the position vector; and ∂ indicates contour.

Another option leading to the same results is to apply the Divergence Theorem in both portions of matrix and void:

$$<\boldsymbol{\varepsilon}> = \frac{1}{2V}\int_{\partial V} (\boldsymbol{u}\otimes\boldsymbol{n} + \boldsymbol{n}\otimes\boldsymbol{u})\, dS. \tag{6}$$

$$<\boldsymbol{\sigma}> = \frac{1}{V}\int_{\partial V} (\boldsymbol{\sigma}\cdot\boldsymbol{n})\otimes\boldsymbol{x} dS. \tag{7}$$

The RVE can be subjected to different boundary conditions, such as uniform kinematic boundary condition resulting from homogeneous strains assumed on the outer surface:

$$\boldsymbol{u} = \boldsymbol{E} \cdot \boldsymbol{x} \qquad \forall \boldsymbol{x} \in \partial V. \tag{8}$$

The void surface is considered to be traction-free.

3 Computational homogenization: influence of morphology on the constitutive response of RVEs under volumetric strains

This section is devoted to study the homogenized constitutive behavior of different RVEs. The first RVE is composed of a sphere with a concentric spherical void. The second one consists of a cube with still a spherical void. The third and last RVE is a cube with a centered cubic void. Therefore, the influence of morphologies of both matrix and voids can be assessed. In addition, for each geometry studied, three porosity levels are considered: (i) $f = 0.001 = 0.1\%$, corresponding to initial defects in metals and alloys; (ii) $f = 0.01 = 1\%$, related to ductile rupture; (iii) $f = 0.1 = 10\%$, aiming to put in clear to evidence possible differences in responses.

All RVEs are subjected to volumetric strains (see Figure 1). In the RVE with spherical external geometry, the uniform kinematic boundary condition derives from homogeneous strains assumed as a hydrostatic strain tensor ($E_m\mathbf{I}$). Therefore:

$$\boldsymbol{u} = \boldsymbol{E} \cdot \boldsymbol{x} = E_m \mathbf{I} \cdot \boldsymbol{x} = E_m \boldsymbol{x} \qquad \forall\, \boldsymbol{x} \in \partial V, \tag{9}$$

where $E_m = E_{kk}/3$ (strain hydrostatic component); $\mathbf{I}$ is the second-order identity; $\boldsymbol{x}$ is the position vector.

Yet the cube-shaped RVE's are subjected to normal displacement on its external faces (see Figure 1) given by:

$$u_1 = E_m x_1,\ u_2 = 0,\ u_3 = 0 \qquad \forall\, x_1 \in \partial V_1 \tag{10}$$
$$u_1 = 0,\ u_2 = E_m x_2,\ u_3 = 0 \qquad \forall\, x_2 \in \partial V_2 \tag{11}$$
$$u_1 = 0,\ u_2 = 0,\ u_3 = E_m x_3 \qquad \forall\, x_3 \in \partial V_3. \tag{12}$$

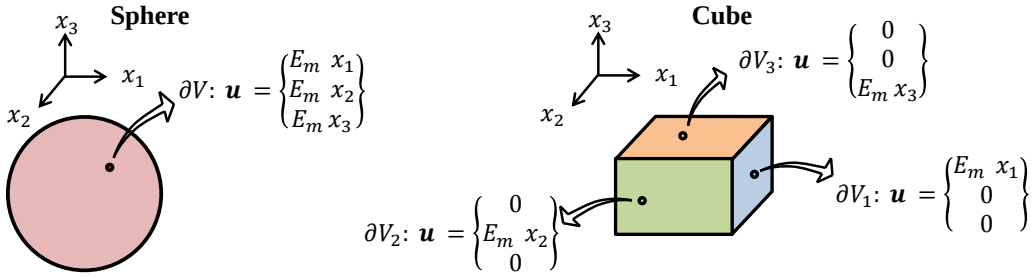

Figure 1. Essential boundary conditions in terms of displacement for spherical and cubic RVE's.

The homogenized response is computationally obtained from the microscopic fields calculated by FEM. In the three-dimensional analyses, meshes of quadratic tetrahedral solid elements with 10 nodes are used. In each case, the stress homogenization is performed by using the following expression considering all finite elements (N_{elem}):

$$\boldsymbol{\Sigma} = \frac{1}{V} \sum_{i=1}^{N_{\text{elem}}} \boldsymbol{\sigma}_i V_i, \tag{13}$$

where $\boldsymbol{\Sigma}$ is the computationally homogenized stress tensor; $\boldsymbol{\sigma}_i$ is the average stress in the element i computed at their integration points; V_i is the volume of the element i; and V is the total volume of the RVE.

Initially, a mesh refinement study was carried out on the hollow spherical RVE by taking as a reference the analytical response of the elastoplastic hollow sphere subjected to uniform radial external displacement. The study was restricted to porosity $f = 0,01 = 1\%$. The meshes used in the refinement are shown in Figure 2, which also indicates data regarding the number of elements, nodes and degrees of freedom. The symmetry and isotropy allowed to consider only 1/8 of the RVEs in order to reduce the computational cost. It is also necessary to define the matrix elastoplastic properties referring to the modulus of elasticity (Y), the Poisson's ratio (ν) and the the microscopic yield stress (σ_0), whose values are respectively: $Y = 200000$MPa, $\nu = 0.3$ e $\sigma_0 = 500$MPa.

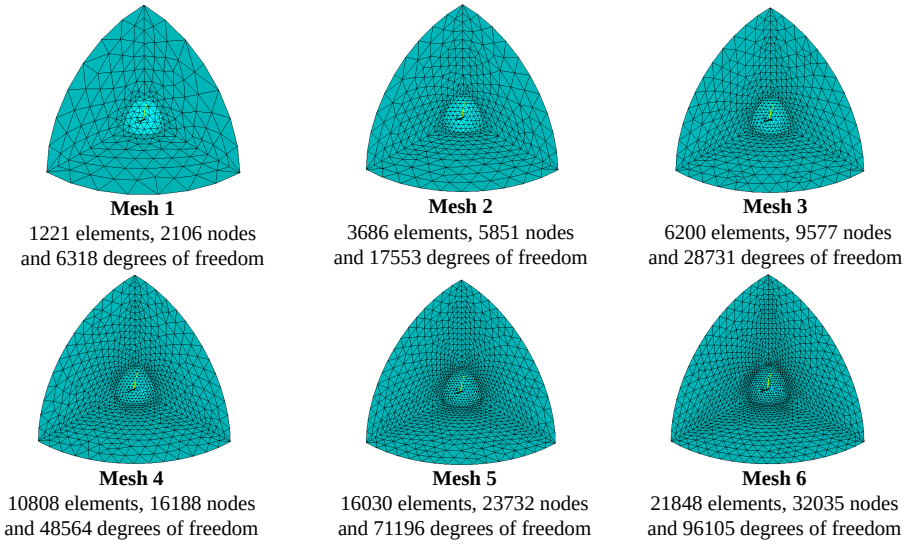

Figure 2. Mesh refining study considering 1/8 of the sphere with spherical void for $f = 0.01 = 1\%$.

Figure 3 exhibits the results of the computationally homogenized hydrostatic stress (Σ_m) for each mesh. For the sake of assessment of accuracy, we compare the computed Σ_m^{comp} with its correspondent exact value obtained from the analytical solution of a perfectly-plastic hollow sphere subjected to external pression: $\Sigma_m^{anal} = -\frac{2}{3}\sigma_0 \ln f$. Follow the expression used to calculate the relative error ($error$):

$$error = \frac{|\Sigma_m^{anal} - \Sigma_m^{comp}|}{\Sigma_m^{anal}} 100\%. \tag{14}$$

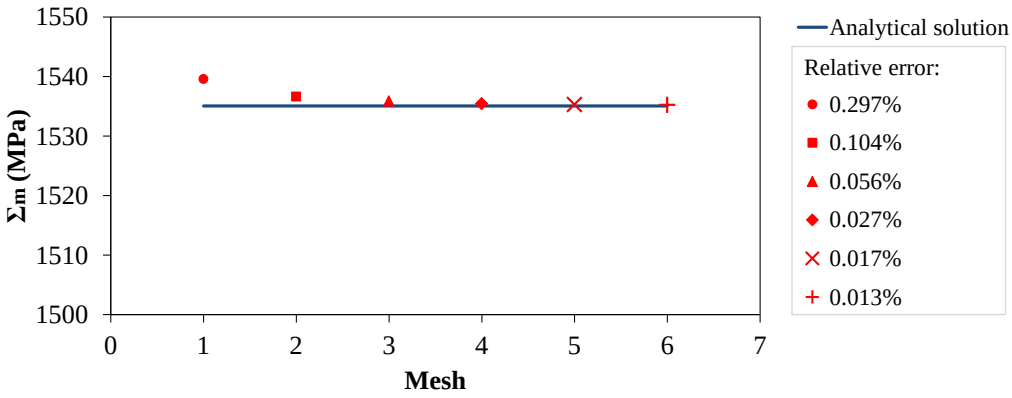

Figure 3. Refinement results considering the sphere with a spherical void for $f = 0.01 = 1\%$.

In general, the differences are small, especially for finer meshes. This highlights the functionality of the homogenization procedure. Reconciling accuracy and computational cost, mesh 5 (16030 elements, 23732 nodes and 71196 degrees of freedom) was used as a reference to the other meshes for the proposed geometries and porosities. The meshes herein studied for $f = 0.1$, $f = 0.01$ and $f = 0.001$ are presented in Figure 4.

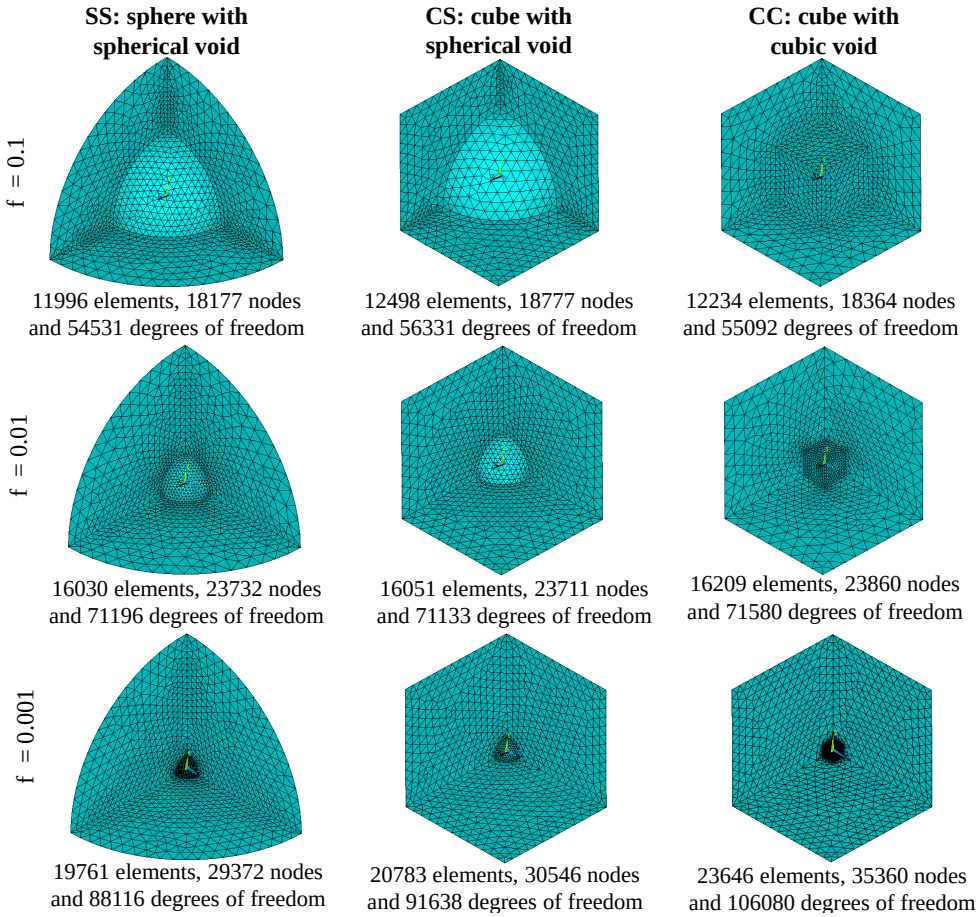

Figure 4. Meshes studied for all RVE's with $f = 0.1$, $f = 0.01$ and $f = 0.001$.

The results for the three porosities hereby studied are shown in the Figure 5. In the Table 1 are shown the final values and also the relative differences of the RVEs with cubic matrix in relation to the RVE formed by the sphere with spherical void. Follows the expressions used to calculate the relative differences ($diff_{CS}$ and $diff_{CC}$):

$$diff_{CS} = \frac{|\Sigma_m^{SS} - \Sigma_m^{CS}|}{\Sigma_m^{SS}} 100\%. \tag{15}$$

$$diff_{CC} = \frac{|\Sigma_m^{SS} - \Sigma_m^{CC}|}{\Sigma_m^{SS}} 100\%. \tag{16}$$

where $diff_{CS}$ is the relative difference of the cube with spherical void; $diff_{CC}$ is the relative difference of the cube with cubic void; Σ_m^{SS} is the result of the sphere with spherical void; Σ_m^{CS} is the result of the cube with spherical void; Σ_m^{CC} is the result of the cube with cubic void.

The spherical RVE with spherical void (SS) presents more strength to the volumetric strain condition. On the other hand, the cubic RVE with cubic void (CC) demonstrates less strength. The RVE with cubic geometry and spherical void shows intermediate strength among the three cases considered. Therefore, for the applied boundary conditions, the optimal material configuration refers to the hollow spherical RVE. This is related to the stress distribution in the microscale (for example, see Figure 6, Figure 7 and Figure 8). Cubic RVE's do not fully plasticize, contributing to a lower homogenized strength of the microstructure. Particularly, for the cubic RVE with cubic void (CC), there is a greater concentration of plastic strains in at internal edges, which generated a loss of strength compared to the case with spherical void. It should also be noticed that the higher the porosities, the more evident the divergences between responses are.

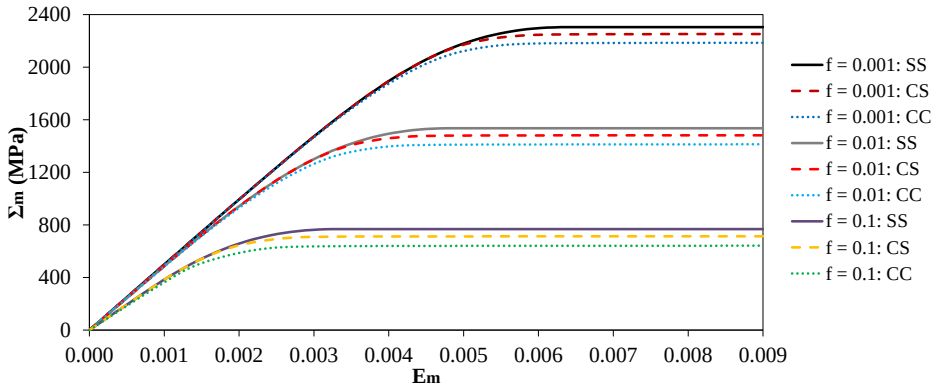

Figure 5. Results of computational homogenization for the different RVEs: sphere with spherical void (SS); cube with spherical void (CS); cube with cubic void (CC).

Table 1. Comparison of the results of computational homogenization for the different RVEs.

f	RVE	Σ_m (MPa)	Relative difference to SS
	SS	767.56	-
0.1	CS	712.85	7.127 %
	CC	641.44	16.430 %
	SS	1535.32	-
0.01	CS	1481.41	3.512 %
	CC	1413.13	7.959 %
	SS	2304.92	-
0.001	CS	2252.26	2.285 %
	CC	2185.54	5.179 %

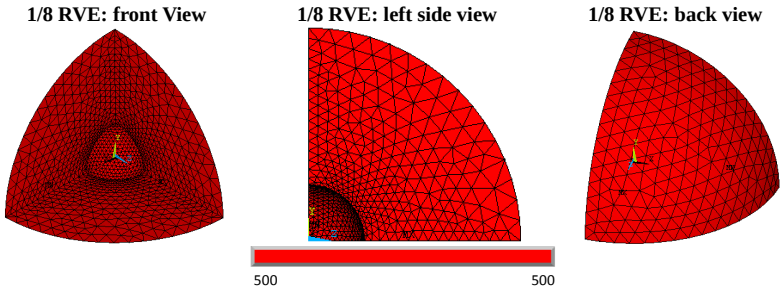

Figure 6. Sphere with spherical void: von Mises equivalent microscopic stress (MPa) for $f = 0.01$.

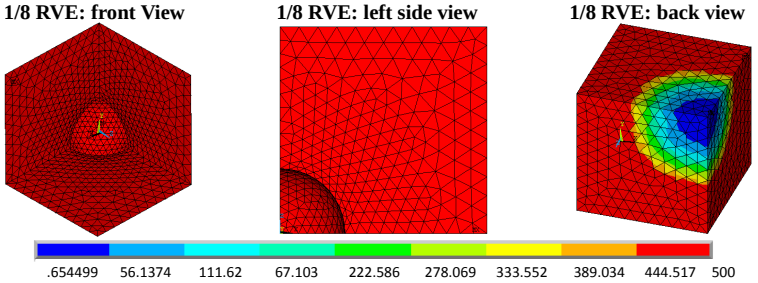

Figure 7. Cube with spherical void: von Mises equivalent microscopic stress (MPa) for $f = 0.01$.

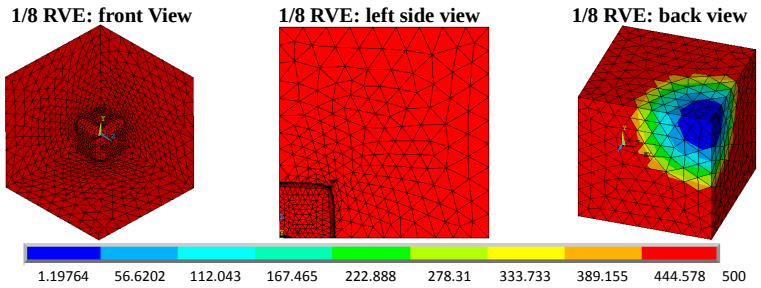

Figure 8. Cube with cubic void: von Mises equivalent microscopic stress (MPa) for $f = 0.01$.

4 Conclusions

In this article, a computational homogenization procedure was used to evaluate the influence of morphology on the constitutive response of RVEs subjected to volumetric strains. In general, it was clear that both the matrix geometry and the void geometry play an important role in the results. When comparing different external morphologies for the matrix, the sphere promotes a more resistant microstructure compared to the cubic ones. When comparing different void morphologies, the homogenized RVE response with cubic void is less strength compared to the RVE response with spherical void. These results reveals the relevance of representing the microstructure with an adequate RVE geometry consistent and increasingly realistic macroscopic rupture responses can be obtained.

Acknowledgements. The authors would like to acknowledge the "Conselho Nacional de Desenvolvimento Científico e Tecnológico – Brasil (CNPq)" and the "Coordenação de Aperfeiçoamento de Pessoal de Nível Superior – Brasil (CAPES) – Finance code 001" for the financial support given to this research.

Authorship statement. The authors hereby confirm that they are the sole liable persons responsible for the authorship of this work, and that all material that has been herein included as part of the present paper is either the property (and authorship) of the authors, or has the permission of the owners to be included here.

References

[1] Fritzen, F., Forest, S., Böhlke, T., Kondo, D., & Kanit, T., 2012. Computational homogenization of elasto-plastic porous metals. *International Journal of Plasticity*, vol. 29, pp. 102–119.
[2] Khdir, Y.-K., Kanit, T., Zaïri, F., & Naït-Abdelaziz, M., 2015. A computational homogenization of random porous media: Effect of void shape and void content on the overall yield surface. *European Journal of Mechanics - A/Solids*, vol. 49, pp. 137–145.
[3] Keralavarma, S. M., 2017. A multi-surface plasticity model for ductile fracture simulations. *Journal of the Mechanics and Physics of Solids*, vol. 103, pp. 100–120.
[4] Carvalho, R. P., Lopes, I. A. R., & Pires, F. M. A., 2018. Prediction of the yielding behaviour of ductile porous materials through computational homogenization. *Engineering Computations*, vol. 35, pp. 604–621.
[5] Dæhli, L. E. B., Hopperstad, O. S., & Benallal, A., 2019. Effective behaviour of porous ductile solids with a non-quadratic isotropic matrix yield surface. *Journal of the Mechanics and Physics of Solids*, pp. 56–81.
[6] Hershey, A. V., 1954. The plasticity of an isotropic aggregate of anisotropic face-centered cubic crystals. *Journal of Applied Mechanics*, vol. 21, pp. 241–249.
[7] Hosford, W. F., 1972. A generalized isotropic yield criterion. *Journal of Applied Mechanics*, vol. 39, pp. 607–609.
[8] Benallal, A., 2017. Constitutive equations for porous solids with matrix behaviour dependent on the second and third stress invariants. *International Journal of Impact Engineering*, vol. 108, pp. 47–62.
[9] Dæhli, L. E. B., Morin, D., Børvik, T., & Hopperstad, O. S., 2017. Influence of yield surface curvature on the macroscopic yielding and ductile failure of isotropic porous plastic materials. *Journal of the Mechanics and Physics of Solids*, vol. 107, pp. 253–283.
[10] Hill, R., 1965. A self-consistent mechanics of composite materials. *Journal of the Mechanics and Physics of Solids*, vol. 13, pp. 213–222.
[11] Mandel, J., 1971. *Plasticité classique et viscoplasticité*. Springer-Verlag, Udine, Italy.